GEOPHYSICAL RESEARCH LETTERS, VOL. 27, NO. 19, PAGES 3061-3064, OCTOBER 1, 2000

Insolation-Weighted Assessment of Northern Hemisphere Snow-Cover and Sea-Ice Variability

R.A. Pielke Sr., and G.E. Liston

Colorado State University, Department of Atmospheric Science, Fort Collins, Colorado

A. Robock

Rutgers University, Environmental Science, New Brunswick, New Jersey

Abstract.
The effects of sea-ice and snow-cover trends on the surface energy budget are assessed by scaling with the direct solar insolation. We have found that, consistent with other studies, an early spring melt has occurred in recent years in the unweighted data, but this trend is muted when the data are weighted by solar insolation. The onset of sea-ice growth and snow in the Fall, however, has no significant trend during the period of record. The effect of sea ice on the reflection of sunlight is largest in May and June when significant sea-ice coverage remains and the sun angle is high. Snow cover, in contrast, has its largest effect on the reflection of sunlight in April.

There have been several effective summaries of low-frequency variability and trends in snow cover and sea ice in the Northern Hemisphere [*Parkinson* 1992; *Robinson et al.,* 1993; *Frei et al.,* 1999; *Huang* 1999; *Johannessen et al.,* 1999; *Parkinson et al.,* 1999; *Robinson* 1999; *Vinnikov et al.,* 1999; *Kuang and Yung* 2000; *Levi* 2000; *Wang and Ikeda* 2000]. *Groisman et al.* [1994] provided an in-depth analysis of the relation between snow cover, temperature, and radiative heat balance over the Northern Hemisphere. These studies, however, did not provide a simple scaling of the direct effect of both the amount of snow-cover and sea-ice extent on the surface incident and reflected solar radiation, which is a function of the time of year. *Robock* [1980] pointed out that to calculate the seasonal and latitudinal cycles of surface reflected radiation, the effects of snow cover and sea ice must be weighted by solar insolation. Here we extend this idea to examine the effects of trends of sea ice and snow cover on the surface energy budget using a scaling by the direct solar insolation. We also investigate the time period through 1998.

In this study, we use Northern Hemisphere monthly snow-covered extent data provided by Dave Robinson of Rutgers University [*Robinson et al.,* 1993; *Robinson* 1999] and Northern Hemisphere monthly sea-ice extent data[1] provided by Bill Chapman and John Walsh of the University of Illinois [*Chapman and Walsh,* 1993].

Paper number 2000GL006127.
0094-8276/00/2000GL006127$05.00

The direct insolation, I, received at a flat portion of the Earth's surface can be estimated from

$$I = S_0 \frac{a^2}{r^2} (\cos Z)\tau, \tag{1}$$

where S_0 defines the solar irradiance at the top of the atmosphere striking a surface normal to the solar beam (S_0 = 1370 W m^{-2}) [*Kyle et al.,* 1985]. The solar zenith angle Z is

$$\cos Z = \sin\delta \sin\phi + \cos\delta \cos\phi \cos\omega, \tag{2}$$

where ϕ is the latitude and ω is the hour angle. The solar declination angle δ, can be approximated by

$$\delta = \phi_T \cos\left(2\pi\left(\frac{d-d_r}{d_y}\right)\right), \tag{3}$$

where ϕ_T is the latitude at the Tropic of Cancer, d is the day number during the year, d_r is the day of the summer solstice, and d_y is the average number of days in a year. The distance of the sun from the Earth at a specific day of the year, a, and the average distance of the Earth from the Sun, r, were defined according to a relationship given in [*Pielke* 1984]. The net sky transmissivity, τ, accounts for the scattering, absorption, and reflection of shortwave radiation within the atmosphere. The increase in transmissivity as the path length through the atmosphere increases, is approximated by

$$\tau = 0.6 - 0.2 \cos Z \tag{4}$$

[*Burridge and Gadd,* 1974]. The diffuse solar irradiance is, of course, also important but was not included in the weighting. This formulation is for clear sky conditions. We acknowledge that significant seasonal cycles of cloudiness and atmospheric transparency (aerosols) also play a role in the solar radiation reaching

[1]The data set for the period 1972-1978 are from the National Ice Center, and from 1979-1998 from the NASA SMMR/DSMP SSMI passive microwave sensors onboard satellites. A grid box was considered ice covered if there was more than a 20% ice concentration (*W. Chapman and J. Walsh 2000*, personal communication).

Table 1. (a) Weighting factors computed for the 15th of each month and applied to the sea-ice extent and snow-covered area observations using a latitude value of 60°N.

Day of Year Mid-Month (Jan-Dec)	Noon Solar Insolation Weight (Normalized by JUN Value)	Daily-Averaged Solar Insolation Weight (Normalized by JUN Value)
15	0.16	0.07
45	0.32	0.17
75	0.54	0.38
105	0.77	0.64
135	0.93	0.88
165	1.00	1.00
195	0.98	0.96
225	0.86	0.77
255	0.66	0.51
285	0.43	0.26
315	0.23	0.11
345	0.13	0.05

the Earth's surface. Such a detailed analysis is beyond the scope of this study.

It is well known that in the Northern Hemisphere, the solar insolation at noon is much less in the middle of the winter than in summer. Thus the influence on the Earth's surface energy budget due to a specific percent change in snow cover/sea ice would be greatest around the summer solstice. Since daylength becomes longer as the summer solstice is approached, both higher midday sun angles, and longer daylight periods enhance the effect of snow cover and sea ice on reflected solar radiation.

By choosing appropriate values of d, ϕ, and ω, the insolation reaching the Earth's surface can be calculated using Eqs. 1-4. Using these equations, we calculated two different weighting factors and used them to assess the seasonal evolution of the radiative impact of snow-covered area and sea-ice extent. These weighting factors are 1) the maximum daily insolation, and 2) the average daily insolation. Our data sets consist of monthly values representing Northern Hemisphere snow-cover and sea-ice extent. Thus, we used values of d that correspond to the 15th of each month. Because we are using data values that represent Northern Hemisphere total areas, and not the spatial distributions of the snow cover and sea ice, we used a generally-representative latitude of 60°N. For our calculations of maximum daily insolation, ω was defined to be solar noon, and for the average daily insolation, ω was varied over the diurnal cycle. Weighting factors were generated by dividing the monthly insolation values by the June value and are provided in Table 1. To highlight how these weighting factors change with choice of latitude, values computed for a latitude of 75°N have also been included in Table 1.

The use of the noontime and average daily solar insolation weighted flux provides a procedure to assess the time periods of the greatest effect of sea ice and snow cover on reflecting sunlight back out into space. From Table 1a, we see that one million square kilometers of snow- and sea-ice cover in December (d = 345), for example, would reflect about the same amount of sunlight at noon as approximately 130,000 square kilometers in June. When the average daily insolation is included,

Table 1. (b) Weighting factors computed for the 15th of each month and applied to the sea-ice extent and snow-covered area observations using a latitude value of 75°N.

Day of Year Mid-Month (Jan-Dec)	Noon Solar Insolation Weight (Normalized by JUN Value)	Daily-Averaged Solar Insolation Weight (Normalized by JUN Value)
15	0.00	0.00
45	0.03	0.00
75	0.32	0.15
105	0.64	0.45
135	0.89	0.81
165	1.00	1.00
195	0.96	0.94
225	0.78	0.63
255	0.49	0.29
285	0.17	0.06
315	0.00	0.00
345	0.00	0.00

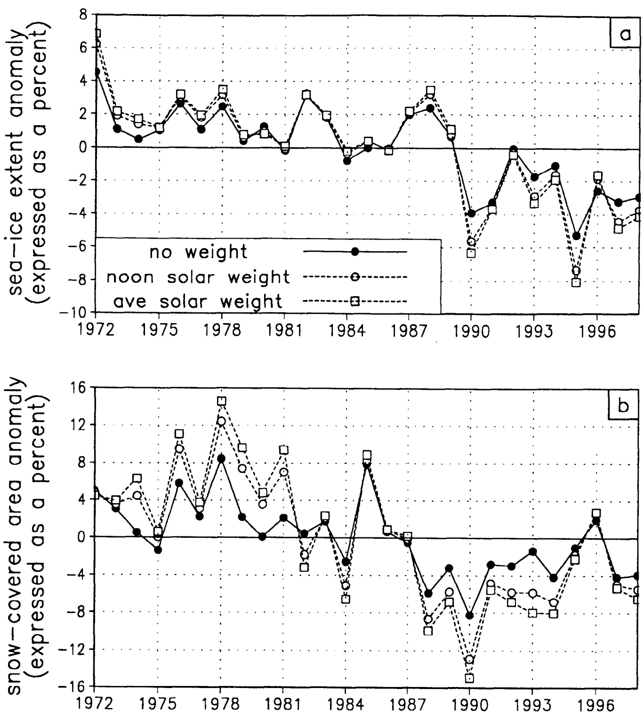

Figure 1. Northern Hemisphere annual-averaged (a) sea-ice extent, and (b) snow-covered area, for the cases no weighting and where the noon solar and average daily solar weighting functions have been applied. Plotted are the values minus the 27-year mean, with that quantity divided by the mean. The sea-ice data were supplied courtesy of William Chapman and John Walsh, University of Illinois (Chapman and Walsh 1993, updated), and the snow-cover data were supplied courtesy of David Robinson, Rutgers University (Robinson et al. 1993; Robinson 1999).

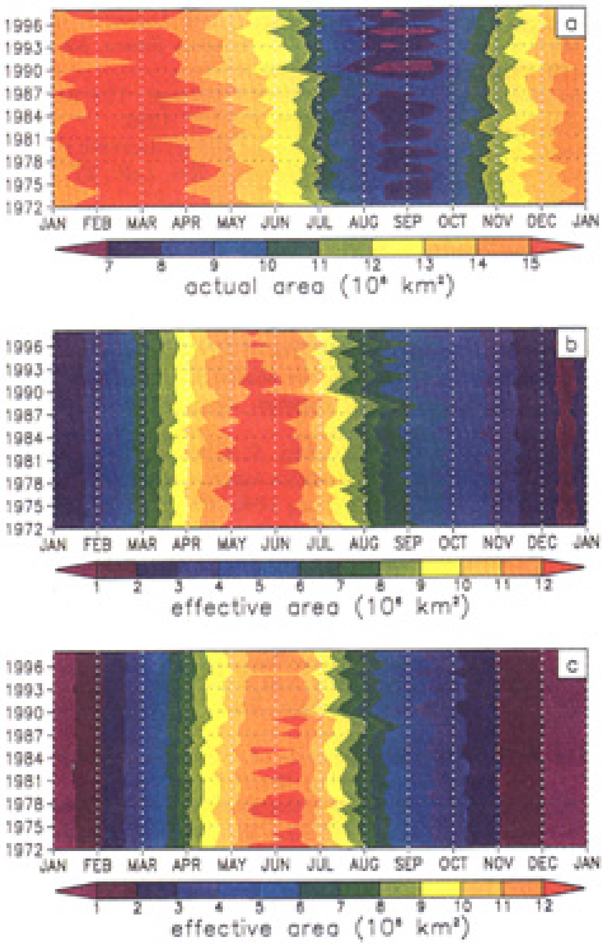

Figure 2. Northern Hemisphere monthly sea-ice extent for the cases of (a) no weighting, (b) noon solar weighting, and (c) average daily solar weighting (weights from Table 1a).

one million square kilometers in December would correspond to 50,000 square kilometers in June.

Figure 1 presents the 1972-1998 sea-ice and snow-cover data as a difference from the long-term mean. Plotted are the observations, and those data when weighted by the insolation weights given in Table 1a. Among the results is that the weighting by insolation produce a somewhat amplified interannual variability. However, the longer-term decline in both sea ice and snow cover, reported by other studies (e.g., [*Vinnikov et al.,* 1999]) is replicated.

Figure 2 and Figure 3 present the unweighted data and the two types of solar insolation weighted data in a Hovmüller-type format where interannual variability can be assessed. The minima in the summer sea ice and snow cover are clearly evident in the Figures. Using the white dashed lines as a reference, it is also clear that an early Spring melt has occurred in recent years in the unweighted data, but this trend is muted when the data are weighted by solar insolation. The onset of sea ice and snow in the Fall, however, has no significant trend during the period of record. The solar insolation weighted data, therefore, also show no Fall trend. The increase of sea ice in the Fall is delayed in recent years, but its influence on trends in the solar insolation weighted flux is minimal.

The analyses of the sea ice and snow cover weighted by the solar insolation show that the effect of sea ice on the reflection of sunlight is largest in May and June when significant sea-ice coverage remains and the sun angle is high. Snow cover, in contrast, has its largest effect in April, consistent with the conclusions of [*Groisman et al.,* 1994]. If the 75°N values from Table 1 are used in these Figures, these same conclusions are reached; the primary difference under this condition is that the winter influence is reduced, leading to more rapid changes from March through May, and July through September (this can be seen by plotting the values in Table 1).

To calculate the actual change in absorbed energy, the albedo of snow or sea ice must be contrasted with that of the underlying surface. The darker the underlying surface, the larger the change in absorbed energy when the snow and sea ice melt. The presence of clouds

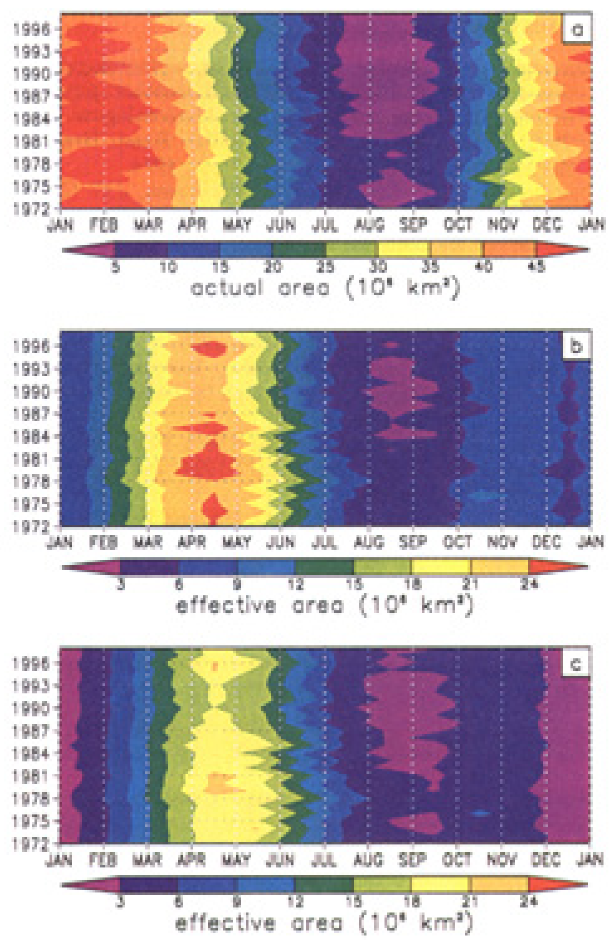

Figure 3. Northern Hemisphere monthly snow-covered area for the cases of (a) no weighting, (b) noon solar weighting, and (c) average daily solar weighting (weights from Table 1a).

and/or aerosols will cause a greater attenuation of the solar irradiance that reaches the surface, so that the change in absorbed solar energy when snow and sea ice are present will be less. Considering the trends in these factors using modern data is the next step in this work, but is beyond the scope of this paper. However, *Robock* [1983], using an energy-balance climate model that did include these factors, showed that the largest amplification of climate change by the positive snow and sea ice/albedo feedbacks occur in the Spring, in agreement with the results shown here.

We recommend that future assessments of trends include evaluations of solar-insolation weighted changes in sea ice and snow cover.

Acknowledgments.
The authors would like to acknowledge support from NASA Grant NAG5-7560, NOAA Grant NA67RJ0152, and the New Jersey Agricultural Experiment Station. We thank Konstantin Vinnikov for valuable comments on the paper. The two Referees (John Walsh and one who remained anonymous) made excellent suggestions which were included in the final version. Dallas Staley very ably completed the typing and editing of the paper.

References

Burridge, D.M., and A.J. Gadd, The Meteorological Office operational 10 level numerical weather prediction model (December 1974). British Meteorological Office Tech. Notes Nos. 12 and 48. London Road, Bracknell, Berkshire, RG12 2SZ England, 57 pp., 1974.

Cavalieri, D.J., P. Gloersen, C.L. Parkinson, J.C. Comiso, and H.J. Zwally, Observed hemispheric asymmetry in global sea ice changes. *Science*, **278**, 1104-1106, 1997.

Cavalieri, D.J., P. Gloersen, C.L. Parkinson, J.C. Comiso, and H.J. Zwally, Deriving long-term series of sea ice cover from satellite passive-microwave multisensor data sets. *J. Geophys. Res.*, **104**, 15803-15814, 1999.

Chapman, W. L., and J. E. Walsh, Recent variations of sea ice and air temperature in high latitudes. *Bull. Amer. Meteor. Soc.*, **74**, 33-47, 1993.

Frei, A., and D.A. Robinson, Northern Hemisphere snow extent: Regional variability 1972-1994. *Int. J. Climatol.*, **19**, 1535-1560, 1999.

Frei, A., D.A. Robinson, and M.G. Hughes, North American snow extent: 1900-1994. *Int. J. Climatol.*, **19**, 1517-1534, 1999.

Groisman, P.Y., T.R. Karl, R.W. Knight, and G.L. Stenchikov, Changes of snow cover, temperature, and radiative heat balance over the Northern Hemisphere. *J. Climate*, **7**, 1633-1656, 1994.

Huang, J., The influence of Arctic and Antarctic ice on southern oscillation. *Acta Meteorologica Sinica*, **13**, 439-449, 1999.

Johannessen, O.M., M. Miles, and E. Bjorgo, The Arctic's shrinking sea ice. *Nature*, **376**, 126-127, 1999.

Kuang, Z., and Y.L. Yung, Observed albedo decrease related to the spring snow retreat. *Geophys. Res. Lett.*, **27**, 1299-1302, 2000.

Kyle, H.L., P.E. Ardanuy, and E.J. Hurley, The status of the Nimbus-7 earth-radiation-budget data set. *Bull. Amer. Meteor. Soc.*, **66**, 1378-1388, 1985.

Levi, B.G., The decreasing Arctic ice cover. *Physics Today*, 19-20, 2000.

Parkinson, C.L., Spatial patterns of increases and decreases in the length of the sea ice season in the North Polar Region, 1979-1986. *J. Geophys. Res.*, **97**, 14377-14388, 1992.

Parkinson, C.L., D.J. Cavalieri, P. Gloersen, H.J. Zwally, and J.C. Comiso, Arctic sea ice extents, areas, and trends, 1978-1996. *J. Geophys. Res.*, **104**, 20837-20856, 1999.

Pielke, R.A., *Mesoscale meteorological modeling.* Academic Press, New York, NY, 612 pp., 1984

Robinson, D.A., Northern Hemisphere snow extent during the satellite era. *Preprints: Fifth Conference on Polar Meteorology and Oceanography*, Dallas, TX, American Meteorological Society, 255-260, 1999.

Robinson, D.A., K.F. Dewey, and R. Heim Jr., Global snow cover monitoring: an update. *Bull. Amer. Meteor. Soc.*, **74**, 1689-1696, 1993.

Robock, A., The seasonal cycle of snow cover, sea ice, and surface albedo. *Mon. Wea. Rev.*, **108**, 267-285, 1980.

Robock, A., Ice and snow feedbacks and the latitudinal and seasonal distribution of climate sensitivity. *J. Atmos. Sci.*, **40**, 986-997, 1983.

Vinnikov, K.Y., A. Robock, R.J. Stouffer, J.E. Walsh, C.L. Parkinson, D.J. Cavalieri, J.F.B. Mitchell, D. Garrett, and V.F. Zakharov, Global warming and northern hemisphere sea ice extent. *Science*, **286**, 1934-1937, 1999.

Wang, J., and M. Ikeda, Arctic oscillation and Arctic sea-ice oscillation. *Geophys. Res. Lett.*, **27**, 1287-1290, 2000.

R.A. Pielke Sr. and G.E. Liston, Colorado State University, Department of Atmospheric Science, Fort Collins, CO 80523 (e-mail: pielke@atmos.colostate.edu; liston@iceberg.atmos.colostate.edu) PHONE/FAX: (970) 491-8293

A. Robock, Rutgers University, Environmental Science, 14 College Farm Road, New Brunswick, NJ 08901 (e-mail: robock@envsci.rutgers.edu) PHONE: (732) 932-9478; FAX: (732) 932-8644

(Received May 16, 2000; accepted July 15, 2000.)